

MHD-KINETIC TRANSITION IN IMBALANCED ALFVÉNIC TURBULENCE

YURIY VOITENKO AND JOHAN DE KEYSER
 Solar-Terrestrial Centre of Excellence, BIRA-IASB,
 Ringlaan-3-Avenue Circulaire, B-1180 Brussels, Belgium
 Draft version October 9, 2018

ABSTRACT

Alfvénic turbulence in space is usually imbalanced: amplitudes of waves propagating parallel and anti-parallel to the mean magnetic field \mathbf{B}_0 are unequal. It is commonly accepted that the turbulence is driven by (counter-) collisions between these counter-propagating wave fractions. Contrary to this, we found a new ion-scale dynamical range of the turbulence established by (co-) collisions among waves co-propagating in the same direction along \mathbf{B}_0 . Co-collisions become stronger than counter-collisions and produce steep non-universal spectra above certain wavenumber dependent on the imbalance. Spectral indexes of the strong turbulence vary around $\gtrsim -3$, such that steeper spectra follow larger imbalances. Intermittency steepens the -3 spectra further, up to -3.7 . Our theoretical predictions are compatible with steep variable spectra observed in the solar wind at ion kinetic scales, but further verification is needed by correlating observed spectra with measured imbalances.

Subject headings: turbulence — waves — solar wind

1. INTRODUCTION

Theory of strong Alfvénic turbulence (Goldreich & Sridhar 1995) predicts that the turbulence cascades anisotropically, mainly toward large perpendicular wavenumbers k_\perp (small perpendicular scales $\lambda_\perp = 2\pi/k_\perp$) across the mean magnetic field, $\mathbf{k}_\perp \perp \mathbf{B}_0$. This prediction has been supported by observations of the solar-wind turbulence (MacBride & Smith 2008, and references therein). With growing k_\perp the turbulent fluctuations become highly anisotropic, $k_\perp \gg k_z$ ($\mathbf{z} \parallel \mathbf{B}_0$), and their perpendicular scales approach the ion gyroradius ρ_i . In this wavenumber range MHD Alfvén waves (AWs) transform into kinetic Alfvén waves (KAWs) (Hasegawa & Chen 1976).

Nonlinear KAW interactions differ significantly from nonlinear AW interactions and produce different turbulent spectra (Voitenko 1998a,b, Schekochihin et al. 2009, Voitenko & De Keyser 2011, Boldyrev & Perez 2012, and references therein). Consequently, at certain sufficiently large wavenumber $k_\perp = k_{\perp*}$ the ion-scale spectral break should occur where the MHD AW turbulence transforms into the KAW turbulence. Recent observations of the solar wind turbulence at ion kinetic scales support this scenario (He et al. 2012, Podesta 2013, Bruno et al. 2014, Roberts et al. 2015). KAW turbulence linked to MHD sources can develop also in solar (Zhao et al. 2013), terrestrial (Moya et al. 2015, Stawarz et al. 2015), and Jovian (von Papen et al. 2014) magnetospheres.

Theories of Alfvénic turbulence are relatively well developed in asymptotic MHD ($k_\perp^2 \rho_i^2 \ll 1$) and kinetic ($k_\perp^2 \rho_i^2 \gg 1$) ranges with perpendicular wavenumber spectra $\sim k_\perp^{-5/3}$ (or $\sim k_\perp^{-3/2}$) and $\sim k_\perp^{-7/3}$, respectively (Goldreich & Sridhar 1995, Gogoberidze 2007, Schekochihin et al. 2009, and references therein). The reference cross-field scale separating MHD and kinetic ranges is the ion gyroradius, $1/k_{\perp*} \sim \rho_i$, because finite- $k_\perp \rho_i$ effects distinguish KAWs from AWs. However, there is debate on the nature of ion-scale spectral break $k_{\perp*}$ and steep spectra at $k_\perp > k_{\perp*}$. Ion gyroradius ρ_i , ion inertial

length δ_i , plasma β , turbulence amplitude B/B_0 , turbulence anisotropy $k_{\perp*}/k_{z*}$, and several their combinations have been suggested as relevant parameters fixing $k_{\perp*}$ (Markovskii et al. 2008, Chen et al. 2014, Boldyrev et al. 2015).

Solar-wind turbulence is imbalanced - amplitudes of waves propagating from the Sun $B_{k(+)}$ are usually larger than amplitudes of sunward waves $B_{k(-)}$, which can affect spectral transport (e.g. Beresniak & Lazarian 2008, Gogoberidze & Voitenko 2016, Yang et al. 2016, and references therein). A common theoretical assumption is that collisions between these counter-propagating Alfvén wave fractions generate turbulence (Howes & Nielson 2013, and references therein). In this Letter, we show that collisions among co-propagating waves (co-collisions thereafter) at $k_{\perp*} < k_\perp < 1/\rho_i$ are stronger than counter-collisions and establish a new dynamical range of the turbulence. We shall refer to this as the weakly dispersive range (WDR). Similarly, we refer to the range $k_\perp \rho_i > 1$, where the kinetic modifications are strong, as the strongly dispersive range (SDR).

2. MODEL AND BASIC RELATIONS

Nonlinear dynamic equation for Alfvén wave amplitudes, including both counter- and co-collisions of waves, has been derived by Voitenko (1998a). Here we construct a semi-phenomenological model for the strong imbalanced Alfvénic turbulence from MHD to kinetic scales using the following approximation for the nonlinear interaction rate:

$$\gamma_{k\pm}^{\text{NL}} = \frac{2+s}{4\pi} k_\perp V_A \Delta_{k,s} \frac{B_{k(\pm s)}}{B_0}, \quad (1)$$

where the wave velocity mismatch $\delta V_{ks}/V_A \equiv \Delta_{k,s} = \sqrt{1 + (k_\perp \rho_T)^2} - s$ and magnetic amplitude $B_{k(\pm s)} = B_{k\pm}$ for co-collisions ($s = 1$) and $B_{k(\pm s)} = B_{k\mp}$ for counter-collisions ($s = -1$). (1) is obtained from equation (6.3) by Voitenko (1998a) assuming local interactions and separating dominant (+) and sub-dominant (-) waves prop-

agating in opposite directions along $\mathbf{B}_0 \parallel \mathbf{z}$. Other definitions are: $\rho_T^2 \simeq (3/4 + T_{ez}/T_{i\perp}) \rho_i^2$ at $k_\perp \rho_i < 1$ and $\rho_T^2 \simeq (1 + T_{ez}/T_{i\perp}) \rho_i^2$ at $k_\perp \rho_i > 1$, T_{ez} - parallel electron temperature, $T_{i\perp}$ - perpendicular ion temperature, $\rho_i = V_{Ti}/\Omega_i$ - ion gyroradius, Ω_i - ion gyrofrequency, $V_{Ti} = \sqrt{T_{i\perp}/m_i}$ - ion thermal velocity, $V_A = B_0/\sqrt{4\pi n m_i}$ - Alfvén velocity.

A simple phenomenological interpretation of (1) can be given in terms of colliding waves 1 and 2. The straining rate experienced by wave 1 in the magnetic shear of wave 2, is proportional not only to the shear $\lambda_\perp^{-1} (B_{k2}/B_0) \sim (2\pi)^{-1} k_\perp (B_{k2}/B_0)$, but also to the relative velocity $V_{ph1} - sV_{ph2}$ defining how fast the wave 1 moves across the shear. Product of these two factors, accounting for locality $k_{\perp 1} \sim k_{\perp 2} \sim k_\perp$ and KAW's dispersion $V_{ph} = V_A \sqrt{1 + (k_\perp \rho_T)^2}$, gives (1) within a factor of order one. The key element of (1) that distinguishes co- and counter-collisions is $\Delta_{k,s}$. Co-collisions ($s = 1$) exist only for finite $k_\perp \rho_T \neq 0$ making $\Delta_{k,s} \neq 0$ and allowing co-propagating waves to move with respect to each other undergoing mutual straining. Counter-collisions ($s = -1$) operate throughout, $\Delta_{k,s} \geq 2$ for all $k_\perp \rho_T \geq 0$, as the counter-propagating waves pass through each other even if they are non-dispersive.

At $k_\perp \rho_T < 1$ (1) reduces to

$$\gamma_{k\pm}^{\text{NL}(\uparrow\uparrow)} = \frac{1}{2\pi} (k_\perp \rho_T)^2 k_\perp V_A \frac{B_{k\pm}}{B_0}, \quad (2)$$

for co-collisions (superscript $\uparrow\uparrow$), and

$$\gamma_{k\pm}^{\text{NL}(\uparrow\downarrow)} = \frac{1}{2\pi} k_\perp V_A \frac{B_{k\mp}}{B_0}. \quad (3)$$

for counter-collisions (superscript $\uparrow\downarrow$).

In SDR, $k_\perp \rho_T > 1$, (1) gives

$$\gamma_{k+}^{\text{NL}(\uparrow\downarrow)} \approx \frac{1}{3} \gamma_{k+}^{\text{NL}(\uparrow\uparrow)} \approx \frac{1}{2\pi} (k_\perp \rho_T) k_\perp V_A \frac{B_{k-}}{B_0},$$

i.e. co-collisions and counter-collisions produce the same scalings.

3. MHD-KINETIC TRANSITION AND SPECTRA

In the asymptotic $k_\perp \rho_T \rightarrow 0$ MHD limit $\gamma_{k\pm}^{\text{NL}(\uparrow\uparrow)} \rightarrow 0$ and the turbulence is driven by counter-collisions, in compliance with Goldreich & Sridhar (1995) and many others. The cascade rate in the dominant component $\gamma_{k+}^{\text{TC}(\uparrow\downarrow)} \sim (B_{k-}/B_{k+})^\mu \gamma_{k+}^{\text{NL}(\uparrow\downarrow)}$, where $\mu = 0, 1/2$, and 1 in the models by Lithwick et al. (2007), Beresniak & Lazarian (2008), and Chandran (2008), respectively. For all μ , the co-collision rate (2) increases with k_\perp faster than $\gamma_{k+}^{\text{TC}(\uparrow\downarrow)}$ and the transition occurs at

$$k_{\perp*} \rho_T \simeq \left(\frac{B_{k*(-)}}{B_{k*(+)}} \right)^{1/2+\mu}. \quad (4)$$

Above this wavenumber, the cascade is controlled by kinetic-type co-collisions.

The turbulence imbalance shifts $k_{\perp*}$ well below $1/\rho_i$ opening window for a new dynamical range WDR $k_{\perp*} < k_\perp < 1/\rho_i$. In what follows we consider the most unfavorable case $\mu = 0$ (Lithwick et al. 2007) with largest $k_{\perp*}$ and narrowest WDR.

3.1. Scaling relations

In the strong turbulence, energy fluxes $\epsilon_\pm = (\gamma_{k\pm}^{\text{NL}(\uparrow\downarrow)} + \gamma_{k\pm}^{\text{NL}(\uparrow\uparrow)}) B_{k\pm}^2 / (4\pi)$ can be presented as

$$\epsilon_\pm \approx \frac{B_0^2 k_\perp V_A}{4\pi} q_k \left(\frac{B_{k\mp}}{B_{k\pm}} + p_k \right) \left(\frac{B_{k\pm}}{B_0} \right)^3, \quad (5)$$

where $q_k = \Delta_{k,-1}$ and $p_k = 3\Delta_{k,1}/\Delta_{k,-1}$ are regular functions growing with k_\perp . Using (5) we express the fluxes ratio as

$$\frac{\epsilon_-}{\epsilon_+} = \frac{\left(1 + p_k \frac{B_{k-}}{B_{k+}}\right)}{\left(\frac{B_{k-}}{B_{k+}} + p_k\right)} \left(\frac{B_{k-}}{B_{k+}}\right)^2. \quad (6)$$

Real solution of this third-order equation for B_{k-}/B_{k+} is straightforward but too cumbersome to show explicitly. Denoting it by b_k , we find from (5) the amplitude scaling $B_{k+} \sim [k_\perp q_k (b_k + p_k)]^{-3}$ and spectrum

$$P_{k+} \equiv k_\perp^{-1} B_{k+}^2 \sim k_\perp^{-1} [k_\perp q_k (b_k + p_k)]^{-6}. \quad (7)$$

At $k_\perp \rho_T < 1$, to the leading order, $p_k \approx 0.75 (k_\perp \rho_T)^2$, $q_k \approx 2$, and the amplitude ratio

$$\frac{B_{k-}}{B_{k+}} \equiv b_k \approx \frac{1}{2} \left(\frac{\epsilon_-}{\epsilon_+} + \sqrt{\left(\frac{\epsilon_-}{\epsilon_+} + 4(k_\perp \rho_T)^2 \right) \frac{\epsilon_-}{\epsilon_+}} \right). \quad (8)$$

Depending on $4(k_\perp \rho_T)^2 \gtrless \epsilon_-/\epsilon_+$, the former "MHD" range $k_\perp \rho_T < 1$ splits into asymptotic MHD range controlled by counter-collisions, and kinetic WDR controlled by co-collisions.

In the asymptotic MHD range $k_\perp \rho_T < 0.5\sqrt{\epsilon_-/\epsilon_+}$ the amplitude ratio (8) is $B_{k-}/B_{k+} \approx \epsilon_-/\epsilon_+$ and (5) gives the amplitude scaling $B_{k\pm} \sim k_\perp^{-1/3}$ and power spectrum $P_{k\pm} = k_\perp^{-1} B_{k\pm}^2 \sim k_\perp^{-5/3}$. These scalings reproduce those reported previously.

In WDR $0.5\sqrt{\epsilon_-/\epsilon_+} < k_\perp \rho_T < 1$, controlled by co-collisions, the amplitude ratio is k_\perp -dependent:

$$b_k \approx \sqrt{\frac{\epsilon_-}{\epsilon_+}} (k_\perp \rho_T). \quad (9)$$

Then $B_{k+} \sim k_\perp^{-1}$ and spectrum

$$P_{k+} = k_\perp^{-1} B_{k+}^2 \sim k_\perp^{-3}. \quad (10)$$

Subdominant amplitudes $B_{k-} \sim \text{const}$ and $P_{k-} \sim k_\perp^{-1}$.

In SDR $k_\perp \rho_T > 1$ we have $p_k \approx 3$, $q_k \approx (k_\perp \rho_T)^2$, then $B_{k\pm} \sim k_\perp^{-2/3}$ and $P_{k\pm} \sim k_\perp^{-7/3}$ in both components.

Evolution of (+) waves in WDR disconnects from (-) waves. As the linear decorrelation rate is $\gamma_k^{\text{L}(\uparrow\uparrow)} \sim \omega_k^{\text{dis}(\uparrow\uparrow)} \approx 0.5k_z V_A (k_\perp \rho_T)^2$ (dispersive part of frequency), $k_{z+} \approx \text{const}$ follows from the critical balance condition $\gamma_k^{\text{L}(\uparrow\uparrow)} \sim \gamma_k^{\text{NL}(\uparrow\uparrow)}$. Evolution of parallel scales is thus suppressed in WDR.

3.2. Non-universal spectra

If WDR is narrow (it is one order or less in the solar wind), the asymptotic spectrum k_\perp^{-3} can hardly set

up. Instead, variable spectra with indexes approaching -3 are expected in WDR. This behavior is observed in Fig. 1 where the spectra (7) are plotted without using asymptotic limits. The spectral indexes in WDR vary $\gtrsim -3$, such that steeper spectra follow larger imbalances ϵ_+/ϵ_- .

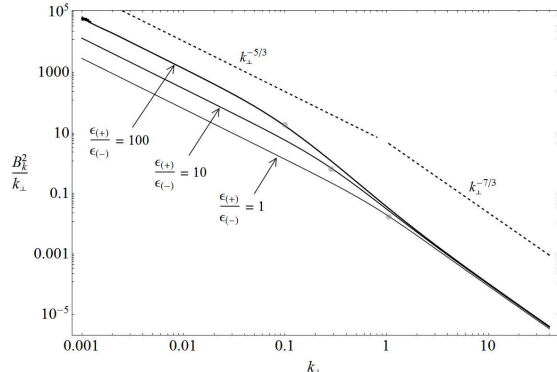


FIG. 1.— Spectra of the dominant (+) component of the strong Alfvénic turbulence (7) for different imbalance ratios $\epsilon_{(+)}/\epsilon_{(-)}$. Grey dots show breaks $k_{\perp*}$ calculated from (4). Perpendicular wavenumber k_{\perp} is normalized by ρ_T , spectral powers are normalized to the same level in SDR kinetic limit. Asymptotic MHD and SDR spectra $-5/3$ and $-7/3$ are shown for reference.

Spectrum of $-$ waves in WDR is much shallower, k_{\perp}^{-1} , which leads to the convergence of $+$ and $-$ spectra. This effect is seen in Fig. 2.

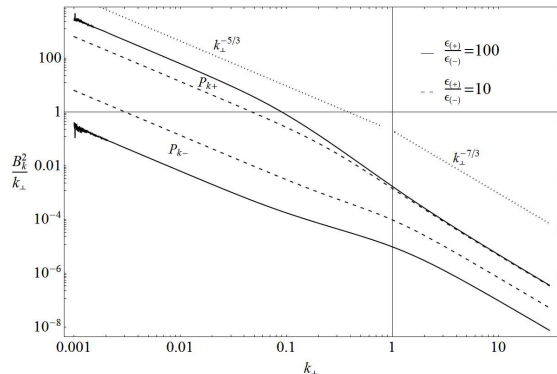


FIG. 2.— Spectra of the dominant (+) and sub-dominant (-) components of the strong turbulence for two imbalance ratios, $\epsilon_{(+)}/\epsilon_{(-)} = 10$ (dashed curves) and 100 (solid curves). The spectra converge stronger for larger imbalance. Other notations as in Fig. 1.

The imbalance of magnetic amplitudes is shown in Fig. 3. The amplitude ratio decreases from $B_{k+}/B_{k-} = \epsilon_+/\epsilon_-$ in the asymptotic MHD range to $B_{k+}/B_{k-} = \sqrt{\epsilon_+/\epsilon_-}$ in the asymptotic kinetic range $k_{\perp} \gg \rho_i^{-1}$. The actual drop of the amplitude ratio is larger than the factor $\sqrt{\epsilon_+/\epsilon_-}$ because co-collisions are already partially operating before $k_{\perp*}$ and after ρ_i^{-1} . Say, if the original imbalance in the asymptotic MHD range is 30, then in the asymptotic kinetic range above $k_{\perp*}$ it drops to about 4, as is seen in Fig. 3 (upper curve).

WDR spectra are affected by intermittency (Boldyrev & Perez 2012, Zhao et al. 2016). The modified spec-

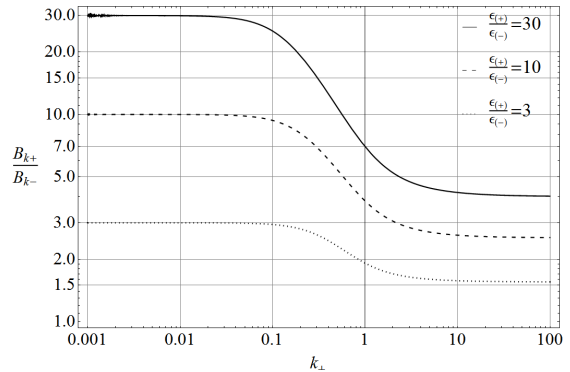


FIG. 3.— Ratio of (+)/(-) magnetic amplitudes for three imbalance ratios, $\epsilon_{(+)}/\epsilon_{(-)} = 30, 10$, and 3 from top to bottom. The amplitude ratio decreases significantly in WDR.

tra can be presented as $\tilde{P}_k \sim k_{\perp}^{-\alpha/3} P_k$, where $\alpha = 1$ for sheet-like and $\alpha = 2$ for tube-like fluctuations (Zhao et al. 2016). The WDR spectrum $P_k \sim k_{\perp}^{-3}$ thus steepens to $\tilde{P}_k \sim k_{\perp}^{-3.7}$, close to the steepest spectra reported by Leamon et al. (1999), Smith et al. (2006), and Sahraoui et al. (2010). Spectra k_{\perp}^{-4} and even steeper can be formed in the weakly turbulent regime (Voitenko 1998b, Galtier & Meyrand 2015).

4. DISCUSSION

Some recent observations are compatible with WDR triggered by imbalance. Bruno et al. (2014) and Bruno & Telloni (2015) have revealed that the ion-scale spectra are systematically steeper in the faster solar winds and suggested it may be caused by Alfvénicity, i.e. imbalance. Our theory supports this suggestion and explains why steeper spectra follow larger imbalances. Chen et al. (2014) have found that at low β the spectral breaks shift to scales larger than ρ_i and associated them with δ_i , which is hard to explain. We suggest that observed break scales can be related not to δ_i , but to $2\pi/k_{\perp*}$ defined by (4). The required imbalances $B_{k+}/B_{k-} = 2.1$ and 3.1 in the models $\mu = 1$ and $1/2$ are realistic; $B_{k+}/B_{k-} = 9.8$ in the model $\mu = 0$ is less realistic. Observed spectral trends (see Fig. 2(a) by Chen et al. (2014) and Fig. 1(b) by Wicks et al. 2011) are the same as in our Figs. 1 and 2, and agree with other WDR properties. Markovskii et al. (2007) argued that the break wavenumber decreases with increasing amplitude at break, which may be caused by the turbulence imbalance (it is usually larger at larger turbulence level). These observations are compatible with our theoretical predictions, but they did not measure imbalances to correlate with spectra. We are not aware of such observations so far.

Kinetic damping at ion scales has been widely discussed as a possible barrier for turbulent cascades (see e.g. Leamon et al. 1999, Voitenko & Goossens 2004, Wu & Yang 2007, Podesta et al. 2010, Maneva et al. 2015, Nariyuki et al. 2014, Cranmer 2014, Passot & Sulem 2015). Nevertheless, nearly universal power-law turbulent spectra $k_{\perp}^{-2.8 \pm 0.3}$ are observed in SDR up to electron gyro-scales (Alexandrova et al. 2013, and references therein). Slight deviations from the theoretical spectra ($k_{\perp}^{-7/3}$ in strong and $k_{\perp}^{-2.5}$ in weak turbulence) can be attributed to intermittency (Boldyrev et al. 2012) and damping (Passot & Sulem 2015). Actu-

ally, Zhao et al. (2016) argued that the damping modifies the spectral index by 0.1 only. This suggests that the damping is not so strong as thought before. In particular, quasi-linear diffusion reduces velocity-space gradients and wave damping (Voitenko & Goossens 2006, Pierrard & Voitenko 2013), which is supported by observations (He et al. (2015)). We thus focused on nonlinear dynamics ignoring linear damping γ_k^L .

Non-universal spectra k_{\perp}^{-2} to k_{\perp}^{-4} observed at $k_{\perp} \lesssim 1/\rho_i$ (Leamon et al. 1999, Smith et al. 2006, Sahraoui et al. 2010) are much steeper than the theoretical spectrum $k_{\perp}^{-5/3}$ formed by counter-collisions. Such strong steepening can hardly be caused by intermittency or damping without significant nonlinear modifications. Our theoretical results uphold the dominant role of nonlinear interactions at ion kinetic scales, where they are strengthened by co-collisions.

5. SUMMARY

We studied the MHD-kinetic transition in strong imbalanced Alfvénic turbulence and found a new dynamical range of the turbulence (WDR) at ion scales. Its main properties are:

1. The MHD-kinetic transition and spectral break in the imbalanced turbulence occur at $k_{\perp*}$ (4), above which the turbulence is controlled by kinetic-type co-collisions. For existing models of the imbalanced MHD turbulence ($\mu = 0; 1/2; 1$) the break $k_{\perp*}$ falls well below $1/\rho_i$ and a

new dynamical range WDR arises at $k_{\perp*} < k_{\perp} < 1/\rho_i$.

2. Turbulent cascade is accelerated in WDR and produce steep non-universal spectra. The spectral index vary from $\gtrsim -2$ to $\lesssim -4$ such that steeper spectra follow larger imbalances, stronger intermittency, or weak turbulence.

3. Magnetic amplitude ratio $B_{k(+)} / B_{k(-)}$ is not scale-invariant in WDR decreasing from ϵ_+ / ϵ_- to $\sqrt{\epsilon_+ / \epsilon_-}$. Similarly, dominant and sub-dominant spectra converge in WDR.

4. Evolution of the parallel wavenumber and frequency slows down in WDR, and wavenumber anisotropy grows faster.

Models with $\mu > 0$ (Beresnyak & Lazarian 2008, Chandran 2008) reproduce the same spectra as in Figs. 1-2 with significantly lower imbalances $B_{k(+)} / B_{k(-)}$ than those required in the $\mu = 0$ model (Lithwick et al. 2007). WDR spectra are steeper than in nearby MHD and SDR ranges, which results in a double-kink spectral pattern. This and other properties of WDR are compatible with observations of the solar-wind turbulence at ion kinetic scales. Applicability of our theory to solar-wind turbulence needs further verifications by correlating observed spectra with measured imbalances.

This research was supported by the Belgian Science Policy Office (through Prodex/Cluster PEA 90316 and IAP Programme project P7/08 CHARM).

REFERENCES

- Alexandrova, O., Chen, C. H. K., Sorriso-Valvo, L., Horbury, T. S., & Bale, S. D. 2013, *Space Sci. Rev.*, 178, 101.
- Beresnyak, A., & Lazarian, A. 2008, *ApJ*, 682, 1070.
- Boldyrev, S., & Perez, J. C. 2012, *ApJL*, 758, L44.
- Boldyrev, S., Chen, C. H. K., Xia, Q., & Zhdankin, V. 2015, *ApJ*, 806, 238.
- Bruno, R., Trenchi, L., & Telloni, D. 2014, *ApJL*, 793, L15.
- Bruno, R. & Telloni, D. 2015, *ApJL*, 811, L17.
- Chandran, B. D. G. 2008, *ApJ*, 685, 646.
- Chen, C. H. K., Leung, L., Boldyrev, S., Maruca, B. A., & Bale, S. D. 2014, *GRL*, 41, 8081.
- Cramer, S. R. 2014, *ApJS*, 213, 16.
- Galtier, S. & Meyrand, R. 2015, *JPlPh*, 81, 325810106.
- Gogoberidze, G. 2007, *PhPl*, 14, 022304.
- Gogoberidze, G. & Voitenko, Y. M. 2016, *Astrophys. Space. Sci.*, 361, 364.
- Goldreich, P., & Sridhar, S. 1995, *ApJ*, 438, 763.
- Hasegawa, A., & Chen, L. 1976, *PhFl*, 19, 1924.
- He, J., Tu, C., Marsch, E., & Yao, S. 2012, *ApJ*, 745, L8.
- He, J., Wang, L., Tu, C., Marsch, E., & Zong, Q. 2015, *ApJL*, 800, L31.
- Howes, G. G., & Nielson, K. D. 2013, *Phys. Plasmas*, 20, 072302.
- Leamon, R. J., Smith, C.W., Ness, N. F., & Wong, H. K. 1999, *JGR*, 104, 22331.
- Lithwick, Y., Goldreich, P., & Sridhar, S. 2007, *ApJ*, 655, 269.
- MacBride, B. T., & Smith, C. W. 2008, *ApJ*, 679, 1644.
- Maneva, Y. G., Vinas, A. F., Moya, P. S., Wicks, R. T., & Poedts, S. 2015, *ApJ*, 814, 33.
- Markovskii, S. A., Vasquez, B. J., & Smith, C. W. 2008, *ApJ*, 675, 1576.
- Moya, P. S., Pinto, V. A., Vinas, A. F., Sibeck, D. G., Kurth, W. S., Hospodarsky, G. B., & Wygant, J. R. 2015, *JGRA*, 120, 5504.
- Nariyuki, Y., Hada, T., & Tsubouchi, K. 2014, *ApJ*, 793, 138.
- Passot, T., & Sulem, P. L. 2015, *ApJL*, 812, L37.
- Pierrard, V., & Voitenko, Y. 2013, *SoPh*, 288, 355.
- Podesta, J. J. 2013, *SoPh*, 286, 529.
- Podesta, J. J., Borovsky, J. E., & Gary, S. P. 2010, *ApJ*, 712, 685.
- Roberts, O. W., Li, X., & Jeska, L. 2015, *ApJ*, 802, 2.
- Sahraoui, F., Goldstein, M. L., Belmont, G., Canu, P., & Rezeau, L. 2010, *PhRvL*, 105, 131101.
- Schekochihin, A. A., Cowley, S. C., Dorland, W., Hammett, G. W., Howes, G. G., Quataert, E., & Tatsuno, T. 2009, *ApJS*, 182, 310.
- Smith, C. W., Hamilton, K., Vasquez, B. J., & Leamon, R. J. 2006, *ApJL*, 645, L85.
- Stawarz, J. E., Ergun, R. E., & Goodrich, K. A. 2015, *JGRA*, 120, 1845.
- Voitenko, Yu. M. 1998a, *JPlPh*, 60, 497.
- Voitenko, Yu. M. 1998b, *JPlPh*, 60, 515.
- Voitenko, Y. & Goossens, M. 2004, *NPGeo*, 11, 535.
- Voitenko, Y. & Goossens, M. 2006, *Space Sci. Rev.*, 122, 255.
- Voitenko, Y. & De Keyser, J. 2011, *NPGeo*, 18, 587.
- von Papen, M., Saur, J., & Alexandrova, O. 2014, *JGRA*, 119, 2797.
- Wicks, R. T., Horbury, T. S., Chen, C. H. K., & Schekochihin, A. A. 2011, *PhRvL*, 106, 045001.
- Wu, D. J., & Yang, L. 2007, *ApJ*, 659, 1693.
- Yang, L., Lee, L. C., Chao, J. K., Hsieh, W. C., Luo, Q. Y., Li, J. P., Shi, J. K., & Wu, D. J. 2015, *ApJ*, 817, 178.
- Zhao, J. S., Wu, D. J., & Lu, J. Y. 2013, *ApJ*, 767, 109.
- Zhao, J. S., Voitenko, Y. M., Wu, D. J., & Yu, M. Y. 2016, *JGRA*, 121, 5.